DOI: https://doi.org/10.37434/tpwj2026.02.01

MATHEMATICAL MODELING OF ELECTRICAL AND THERMAL PROCESSES IN A GRAPHITIZED CORED ELECTRODE FOR ALTERNATING CURRENT ARC STEELMAKING FURNACES

I.V. Krivtsun, S.V. Rymar, O.G. Bogachenko, I.O. Honcharov, I.O. Neilo, R.S. Hubatyuk, O.T. Zelnichenko

E.O. Paton Electric Welding Institute of the NASU
11 Kazymyr Malevych Str., 03150, Kyiv, Ukraine

ABSTRACT

The results of mathematical modeling of electrical and thermal processes in a graphitized cored (composite) electrode for alternating current arc steelmaking furnaces are presented. A comparison is made with similar processes in a monolithic electrode and the regularities of these processes are determined. The calculations are performed using the developed mathematical model based on the finite element method with the introduction of a number of simplifications and assumptions. The distribution of current density, electric potential, magnetic induction and temperature in the electrode is studied, which allows predicting the operation of cored electrodes in arc furnaces. The estimated results of the calculations show that cored electrodes, when operating on alternating current, similar to direct current operation, are also characterized by lower electrical losses and heating temperatures compared to monolithic electrodes, which makes them more energy and resource efficient.

KEYWORDS: cored (composite) electrodes, monolithic electrodes, arc steelmaking furnaces, alternating current, current density distribution, electric potential distribution, temperature distribution, energy efficiency, resource efficiency

INTRODUCTION

This work is a logical continuation of paper [1], which deals with electrical and thermal processes in graphitized cored (composite) electrodes for steelmaking direct current arc furnaces. This paper considers similar processes, but for electrodes of alternating current furnaces. This is natural, as 80 % of arc steelmaking furnaces in the world use exactly the alternating current [2]. The capacity of such furnaces is equal to 15–180 t of steel.

As electric steel production is extremely resource- and energy-intensive, extension of the service life of the high-cost graphitized electrodes and reduction of electrical energy consumption provides a significant resources saving and reduction in the negative environmental impacts of the steel melting process. Also important is saving the high-cost materials, such as ferroalloys and alloying substances. Practical experience of using graphitized cored electrodes, which had been invented and developed at PWI for the first time, proved their positive role in solving the above problems [2–4] in industrial AC electric arc furnaces of 6–50 t capacity [5, 6].

The cored (composite) electrode being considered is similar to the monolithic graphitized electrode, but it has a through hole along the axis of symmetry, densely filled with materials containing chemical elements with a low work function of electrons [3, 4]. This is the core.

Not all the studies of electrode functioning can be conducted directly on operating industrial furnaces, in connection with the high temperatures in them. Therefore, it is rational to perform a number of investigations using the modern methods of mathematical modeling of the electromagnetic and temperature fields to enable further prediction of the physical-chemical and diffusion processes in the core-electrode system and in the arc working zone [7–9] and other processes.

The purpose of the work is determination of the main regularities of the electromagnetic and thermal processes taking place in graphitized cored electrodes for steelmaking AC arc furnaces.

The objective of the work is development of mathematical models and performance of modeling of electromagnetic and temperature fields propagation in the cored and monolithic electrodes, through which the alternating electric current of industrial frequency is flowing. Calculations are required for investigation and prediction of processes occurring in cored electrodes of steelmaking AC arc furnaces and determination of the influence of these processes on the technical and economic indices of steel melting, compared to monolithic electrodes.

In terms of methodology, the work is based on the regularities of propagation of the electromagnet-

ic and temperatures fields, using Maxwell equations for the electromagnetic part of the problem, Fourier equations, allowing for thermal radiation and convective heat exchange from the surface into the environment for the thermal part of the problem, and Joule–Lentz law, which combines both the parts of the problem. Finite element method is used, which combines the integral characteristics with the characteristics of the studied electromagnetic and temperature fields. The skin-effect is taken into account, which even though slightly, but is still manifested in the significantly heated areas of the studied electrodes, in connection with an increase in electrical resistance of the electrode body graphite. Temperature dependence of the material thermal-physical characteristics is taken into account.

The work should result in deriving the computed patterns of the distribution of current density, electric potential, magnetic induction and temperature in the cored and monolithic electrodes in the case of their heating from the start of the process and in a stationary mode, and revealing the main regularities of their distribution.

The originality of the work consists in the conducted research of the distributions of the current density, electric potential and temperature in the cored electrode, which allows predicting the operation of such electrodes in steelmaking AC arc furnaces.

Practical importance of the work consists in the possibility to determine by mathematical modeling the tendencies of the influence of cored electrodes on the energy, technological and economical components of the working process of the steelmaking arc furnaces.

In this connection, it is relevant to study the electromagnetic and thermal processes in the graphitized cored electrodes, in case of their operation on commercial frequency alternating current.

When plotting the mathematical models, the following simplifications and assumptions were taken in order to perform approximate calculation of the electromagnetic and thermal processes in the graphitized and monolithic electrodes. *First,* the processes in the arc were not considered. *Second*, the electric contact of the current conduit with the electrode was considered ideal, without allowing for contact resistance, depending on the electric field intensity, current density and volumetric heat release. *Third,* the temperature of furnace gases around the electrode and the furnace wall temperature along their height were assumed to be such which change linearly; and the temperature on the molten slag surface is constant; temperature of the arc active spot at the electrode tip, contacting the cathode or anode region of the arc in the case of the current polarity change in each of its half-periods, was set as a constant and averaged value between the temperatures of the cathode (lower temperature) and anode (higher temperature) of the spots under the conditions of the arc supply by direct current of reverse or straight polarity, respectively. This is admissible as the characteristic time of the temperature change at a massive electrode tip is much greater than the characteristic time of current polarity change for the 50 Hz industrial frequency of current, supplied to the arc. To confirm this, we will write the Fourier differential equation, for instance along coordinate r (electrode radius for an axisymmetric task):

$$\gamma C_p \frac{\partial T}{\partial t} = \frac{1}{r}\frac{\partial}{\partial r}\left(\lambda r \frac{\partial T}{\partial r}\right),$$

where γ is the material density; C_p is the specific heat capacity of the material; T is the temperature; t is the time; λ is the heat conductivity.

This equation can be presented in the form of a record for the growth of functions and arguments:

$$\gamma C_p \frac{\Delta T}{\Delta t} = \frac{1}{r}\frac{1}{\Delta r}\left(\lambda r \frac{\Delta T}{\Delta r}\right),$$

from where the time increment

$$\Delta t = \frac{\gamma C_p}{\lambda}\Delta r^2.$$

The latter formula is the base of the Fourier criterion.

Δt value can be interpreted as a characteristic time of the change of electrode material temperature. For a graphitized electrode from 10 to 200 mm in diameter and its temperature from 20 to 4000 °C this value can be in the time range of the order of $1–10^4$ s, and the change in the cathode and anode spots at the electrode tip for 50 Hz current frequency occurs during a much shorter characteristic time of 10^{-2} s.

Fourth, as the diffusion processes in the core-electrode system are still at the research stage, they were so far considered as cases of insignificant diffusion of elements which is indirectly taken into account by a certain change in the specific electrical resistances of the electrode and the core under the impact of temperature. All the other electrical and thermal-physical parameters did not depend on temperature. *Fifth*, the electric current path was selected through the entire conditionally stationary surface of the arc active spot on the electrode lower tip. *Six*, a single electrode is considered, which is separated from the three-electrode system of the furnace [2, 6, 10]. That is, the combined action of the magnetic fields of a three-phase system of power supply to the current-carrying conductors (electrodes), is not taken into account, and the effect of closeness and Lorentz force, which in the

three-phase system is the cause for an axisymmetric burn-out of the electrode tips relative to the vertical axis of symmetry, is not allowed for, accordingly. In a separated single electrode the burn-out of its tip is symmetrical, which enables solving the problem in an axisymmetric representation. This simplification allows facilitating the comparison of the influence of alternating and direct currents on separated electrodes [1] in the case of their similar effective values and the same overall dimensions of the electrodes. *Seven*, as the conduction current in the conductor (electrode) is significantly higher than the bias current, the later can be neglected.

INVESTIGATION RESULTS

MATHEMATICAL MODEL EQUATIONS

We will write the Maxwell's general basic equations for the electromagnetic problem (of the electric and magnetic fields), which are used in mathematical modeling:

$$\nabla\mathbf{J} = 0;\ \nabla\times\mathbf{H} = \mathbf{J};\ \mathbf{J} = \sigma\mathbf{E};\ \mathbf{E} = -\nabla V - j\omega\mathbf{A};\ \ \mathbf{B} = \nabla\times\mathbf{A},$$

where ∇ is the Nabla operator; **J** is the current density vector; **H** is the magnetic field intensity vector; σ is the specific electrical conductivity of the material, $\sigma = 1/\rho$; ρ is its specific electrical resistance; **E** is the electric field intensity vector; $j = \sqrt{-1}$ is the conditional unit; ω is the angular frequency of the current; V is the scalar electric potential; **A** is the vector magnetic potential; $\mathbf{B} = \mu_0\mu_r\mathbf{H}$ is the magnetic induction vector; μ_0 is the magnetic constant; μ_r is the relative magnetic permeability of the environment.

The Ampere's law and conservation of current is also used:

$$\nabla\times(\mu_0^{-1}\mu_r^{-1}\mathbf{B}) + \sigma\nabla V + j\omega\sigma\cdot\mathbf{A} = 0.$$

We will white the boundary conditions for the electric and magnetic fields. *First,* the electric (except for surfaces of current supply and removal) and magnetic isolation of the computational region, including the closed region of the gas environment around the electrode between the surfaces of current supply and removal:

$$\mathbf{n}\cdot\mathbf{J} = 0;\ \mathbf{n}\cdot\mathbf{A} = 0,$$

where **n** is the unit normal vector.

Second, the electric potential on the upper terminal $V = 0$. Current value I_0, flowing in the electrode (amplitude value for alternating current) is assigned at the arc active spot on the electrode lower tip.

Fourier equation for a nonstationary (time variable) thermal problem, which describes the temperature field distribution for heat exchange in the electrode:

$$\gamma(T)C_p(T)\frac{\partial T}{\partial t} - \nabla[\lambda(T)\nabla T] = Q,$$

where Q is the specific power of the heat sources (during the body heating by electric current the distribution of volume heat release in it $Q = \mathbf{J}^2/\sigma$). Parameters γ, C_p, λ here depend on temperature T.

The first term determines the nonstationarity of the heat exchange process, the second determines heat transfer due to heat conductivity.

In the case of a stationary problem, the first term in this expression will be equal to zero, and it will disappear from the equation.

The region of the gas environment around the electrode between the surfaces of current supply and removal is not involved in the thermal problem.

Boundary conditions for the thermal problem are as follows. *First,* the condition of the 1st kind applies to the arc active spot on the electrode tip lower surface — the isothermal condition of a constant value of temperature: for monolithic electrode $T_0 = 4440$ °C [8]; for the cored electrode $T_0 = 4000$ °C. For the cored electrode the temperature value was calculated from the relationship of arc temperatures for the monolithic [11] and cored [12] electrodes, where the temperature of the cored electrode arc is by 15–20 % lower than that of the monolithic electrode arc. An assumption was made that the temperature of the arc cathode spots for such electrodes has approximately the same difference [1], and for the cathode-anode arc spots it is smaller – 10–15 %. *Second,* a condition of the 3rd kind applies over the total electrode surface area, except for the arc active spot, which allows for heat dissipation q_h due to convective heat exchange with the environment

$$-\mathbf{n}\cdot[-\lambda(T)\nabla T] = \alpha(T_{ext} - T) = q_h.$$

Here, α is the convective heat exchange coefficient which can be set differently on different regions of the surface; T_{ext} is the ambient temperature, which can be different in different parts of the electrode.

Third, to allow for the radiation heat losses q_ε over the entire electrode surface area, expect for the arc active spot, condition of the third kind is applied, and the following expression is assigned:

$$-\mathbf{n}\cdot[-\lambda(T)\ \nabla T] = \varepsilon\delta(T_{amb}^{\ 4} - T^4) = q_\varepsilon,$$

where ε is the Stephan–Boltzmann constant; δ is the surface emissivity; T_{amb} is the temperature of the surfaces, exposed to the beams from the radiating body.

In the stationary thermal mode of the furnace, the averaged temperature of molten slag is equal to 1620 °C; temperature of furnace gases in the region of the electrode lower side surface is 2500 °C, and in the zone of the upper side surface of the electrode in the furnace vault it is 1800 °C; temperature of the surface of the furnace side wall above the molten slag

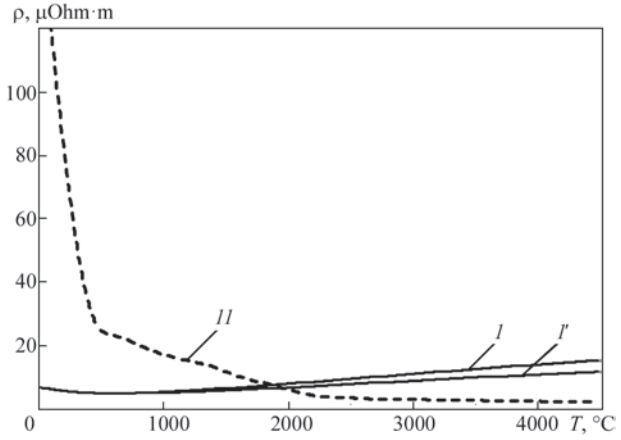

Figure 1. Dependences of specific electrical resistances ρ on temperature *T*: *1* — monolithic graphitized electrode; *1′* — graphitized part (body) of the cored electrode, where diffusion processes took place in the core-electrode system; *11* — core of an experimental composition No. 11 [1]

is 1700 °C; temperature of the surface of the furnace side wall near the vault is 1500 °C.

Figure 1 gives the dependencies of specific electrical resistances ρ on temperature *T*: *1* — monolithic graphitized electrode for: *1′* — graphitized part (body) of the cored electrode, in which certain diffusion processes occurred in the core-electrode system, which reduced its specific electrical resistance, compared to the monolithic electrode resistance; *II* is the core of experimental composition No. 11 [1] with elements with a low work function of electrons [2–4].

One can see from Figure 1 that up to the temperature of approximately 1900 °C the value of the core resistance is greater than electrode resistance *1′*, and it decreases with temperature rise. At high temperatures the core becomes more electrically conductive than the graphitized body of the electrode and the electrical losses in significantly heated regions of the cored electrode become smaller than the losses in similar regions of the monolithic electrode.

CASE OF ELECTRODES SEPARATED FROM THE FURNACE AND THE ARC

In order to analyze the temperature field in the cored electrode in the case of an alternating electric current flowing through it and to compare it with the monolithic electrode, let us first consider the case, when the electric current flows through electrodes separated from the furnace and the arc, which are located in open air with 20 °C temperature. The electric current is supplied between the contact of the upper current conduit (electrode holder) and contact-simulator of the dimensions of the arc active spot at the electrode lower tip. The first boundary condition of the thermal problem changes from the isothermal one of the 1st kind to a homogeneous adiabatic condition of the second kind, when the area of contact with the arc active spot dimensions is thermally insulated and the thermal flow does not pass through it.

For a commercial cored electrode being considered, the diameter of the through hole for its filling with the core is equal to 50 mm. For the conducted modeling it is taken that the cored and monolithic electrodes have the same shape, as the electrodes in the furnace, for which the diameter (225 mm) in the lower part is smaller than the initial diameter (350 mm) in the upper part in connection with the electrode burnout. The height of the system of electrodes in the furnace (electrode candles) was assumed to be 3680 mm. The approximate calculated distance from the electrode lower tip to the furnace vault and to the lower tip of the upper current supply is equal to 2530 and 2820 mm, respectively. The height of the upper current supply (electrode holder) is 500 mm. A variable sinusoidal current with the effective value of 11 kA flows through the electrodes for all the calculation options. The diameter of the contacts simulating the active arc spot for a cored electrode is taken to be 115 mm, and for the monolithic electrode it is 50 mm. The electrode sections are connected to each other by monolithic graphite nipples with specific resistances 15 % lower than that of a monolithic graphitized electrode and by 5 % lower for the lower nipple, which is exposed to high temperatures in the furnace for a longer time, and in which diffusion processes between it and the electrode have taken place.

Considered is an axisymmetric problem in a system of coordinates with axes 0, *z* and 0, *r* (*z* is the vertical axis in the axial direction, *r* is the horizontal axis in the radial direction) with graphic representation of half of the computational region from the vertical axis of symmetry in the Figures.

Figure 2, *a* shows a computational distribution of the temperature field in the cored electrode in the case of its heating by 11 kA current in open air with 20 °C to a stable temperature after two hours, and Figure 2, *b* presents 4 pairs of temperature distributions along the electrode height (coordinate *z*) on the electrode axis of symmetry (greater temperature in the pairs) and on the straight side surface (lower temperatures in the pairs) with a 30 min step. Figure 2, *c*, *d* shows similar temperature fields in the monolithic electrode. In Figure 2, *a*, *c* the conditional boundary of the arc active spot (contact-simulator boundary) is marked by a line below the electrode tip.

During operation in an alternating current furnace the working surface of the cored electrode tip takes on a characteristic concave dome-shaped form with upward-curved ends, which is due to the through hole with the core. In a monolithic electrode the tip is convex. This is due to the fact that the arc of the cored

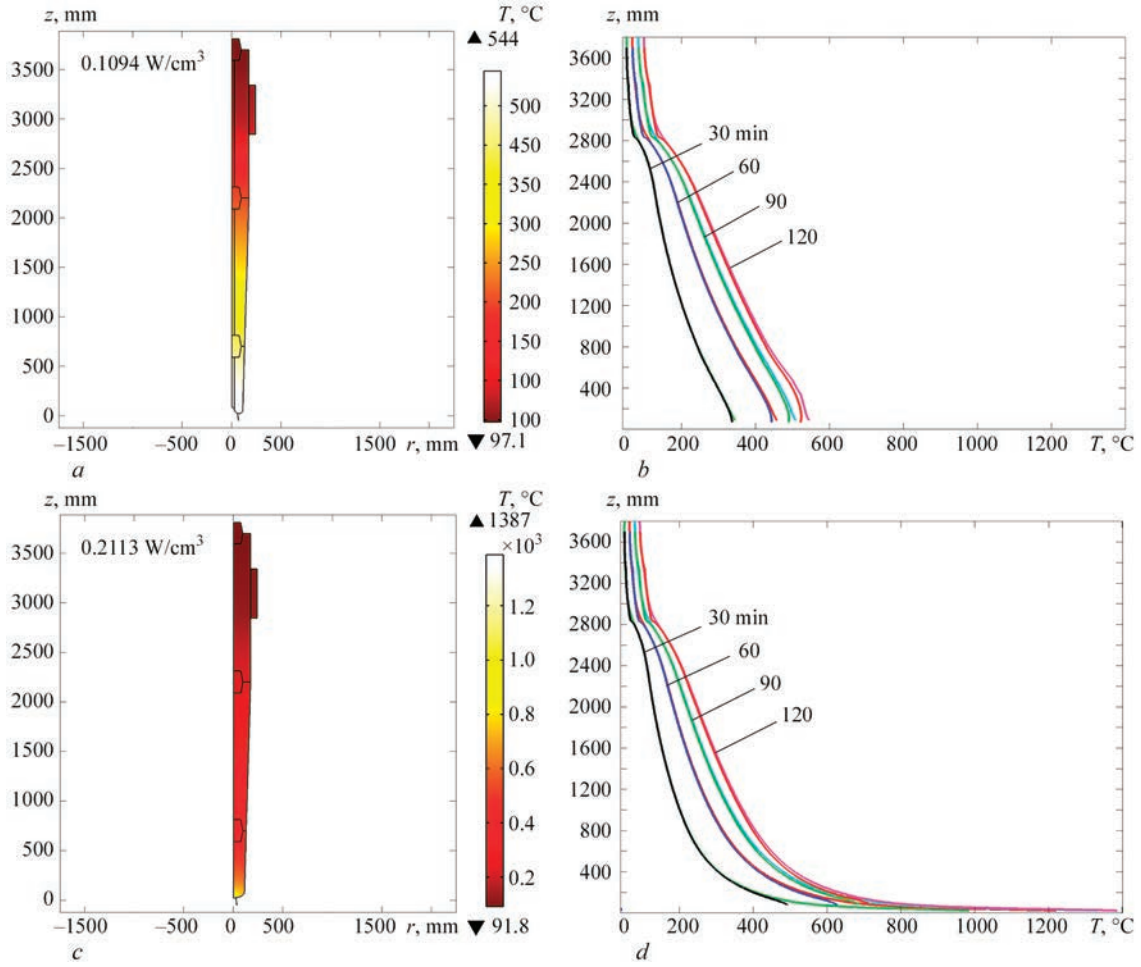

Figure 2. Temperature field in the cored electrode when heated by passing current of 11 kA in open air from 20 °C to a stable temperature after 2 h (*a*) and 4 pairs of temperature distributions along the electrode height (coordinate *z*) on the electrode axis of symmetry (higher temperatures in the pairs) and on the rectilinear side surface (lower temperatures in the pairs) with a 30 min step (*b*), and similar data for the monolithic electrode (*c*) and (*d*)

electrode differs significantly from the monolithic electrode arc by its geometrical and electrical parameters. The AC core arc is defocused, and its diameter is approximately equal to 1/2–3/4 of the electrode tip diameter. It is highly stable in a broad range of lengths and current loads, elastic and spatially stable, concentrated practically in one place and does not migrate over the electrode tip, it is characterized by a high thermal inertia and lower temperature and density of current, compared to the monolithic electrode arc. Now, in the monolithic electrode the arc is concentrated, the arc active spot is small-sized and migrates continuously over the electrode tip surface, burning it out and overheating the melt surface, leading to intensification of evaporation of the main and alloying elements from it. Accordingly, the current in the area of the active arc spot in cored electrodes flows more uniformly due to a larger area of the active spot. Its density is only slightly higher than the current density in the electrode body and heating of the electrode lower part by current is not as significant, as in the monolithic electrode, where the current is concentrated in the arc active spot of a small area.

In the case of electrodes separated from the furnace and the arc, a more than double the difference in the temperatures of the cored — 544 °C (Figure 2, *a* and *b*) and monolithic — 1387 °C (Figure 2, *e* and *f*) electrodes is observed in their lower parts. During modeling the lower contact simulating the arc active spot, is stationary and it does not take into account the spot movement for the monolithic electrode. This yields a somewhat higher temperature, but the tendency to temperature distribution is preserved. The general specific resistive electrical losses in the entire volume of the cored electrode in Figure 2, *a* (from the upper tip of the electrode holder to the lower tip of the electrode) are equal to 0.1094 W/cm^3, and those in the monolithic electrode in Figure 2, *c* are 0.2113 W/cm^3. Two times greater losses in the monolithic electrode are due to higher current density in the electrode lower part (in the contact-simulator zone).

Thus, in the case of electric current flowing through the electrodes, located in open air, the electrical losses and temperatures in the cored electrode are practically two times lower than those in the monolithic electrode. This allows predicting a higher energy efficiency of cored electrodes than that of monolithic ones, as well as lower burnout of cored electrodes and their greater resource efficiency.

CASE OF THERMAL INFLUENCE OF THE ACTIVE ARC SPOT, MELT SURFACE, FURNACE GASES AND FURNACE WALLS ON THE ELECTRODE

Further on we will consider the established thermal modes in the case of the influence of the abovementioned factors on the electrode.

Figure 3, *a* shows the calculated temperature field in the cored electrode, and Figure 3, *b* presents the temperature dependencies along the electrode height (coordinate *z*) along the electrode axis of symmetry (curve *1*) and on the straight side surface (curve *2*). Figure 3, *c* and *d* gives similar dependencies for a monolithic electrode (*c*) and (*d*). Comparing these dependencies one can see that the temperature distributions in the electrodes up to tentatively, 1900 °C are very close, although in the cored electrode the temperature is slightly higher, as the specific electrical resistance of the core (Figure 1) up to the temperature of 1900 °C is higher than that of the graphitized electrode body and heat release in the cored electrode is higher in its greater part. Above the 1900 °C temperature the specific electrical resistance of the core becomes smaller than that of the graphitized electrode body and the heat release in the electrode becomes smaller, as in the case of the monolithic electrode.

In the monolithic electrode the higher temperature values are recorded in the zone of a small-sized active spot of the arc, where the current is directed, causing significant changes in its density and intensive heating of this electrode zone. The temperature of the arc active spots also makes a significant contribution into the temperature level in the electrode tips. As the area of the arc active spot in the cored electrode is not much smaller than that of the electrode tip the heat flows from it heat the electrode tip to a considerable depth. However, the temperature of the arc active spot

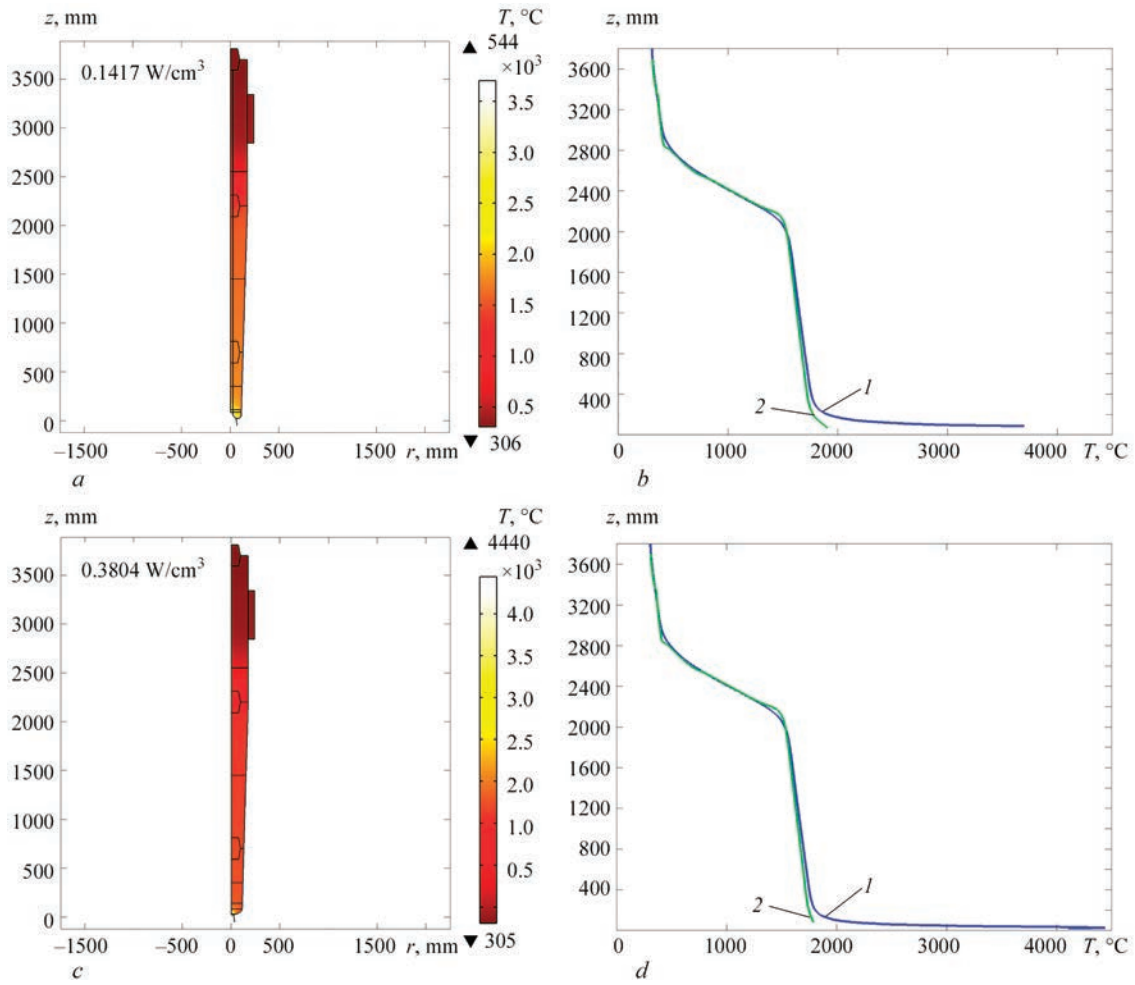

Figure 3. Temperature field in the cored electrode (*a*) and temperature dependences along the electrode height (coordinate *z*) on the electrode axis of symmetry (curve *1*) and on the rectilinear side surface (curve *2*) (*b*); similar data for the monolithic electrode (*c*) and (*d*)

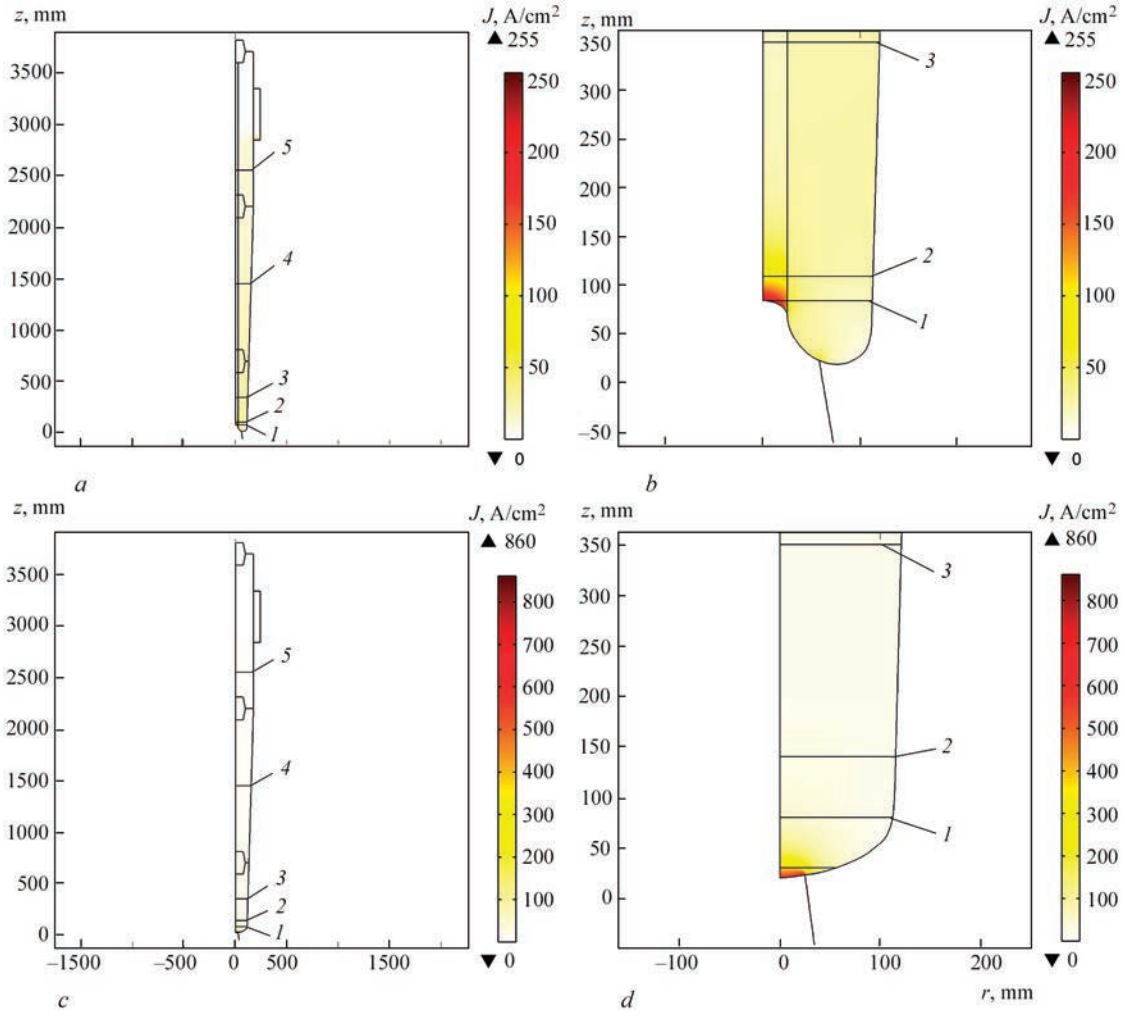

Figure 4. Distribution of current density in the cored electrode (*a*) and magnified image of the electrode tip (*a*), similar data for the monolithic electrode (*c*) and (*d*)

proper of these electrodes is smaller than that of the monolithic electrode spot. Figure 3 illustrates the increase in the temperature values at the electrode tips.

More than 2.5 times greater specific resistive electrical losses of 0.3804 W/cm^3 (Figure 3, *c*) are observed in the total volume of the monolithic electrode, compared to those for cored electrode of 0.1417 W/cm^3 (Figure 3, *a*).

Let us consider the pattern of distribution of the effective values of current density in the electrodes.

Figure 4, *a* shows the distribution of current density in the cored electrode, and Figure 4, *b* is an enlarged image of the electrode tip. Figure 4, *c* and *d* are the same for the monolithic electrode. One can see that the current density distribution in the electrodes correlates with their specific electrical resistances for different temperatures (Figure 1). In regions with a greater value of the core resistance the current density is smaller, than in the body of the electrode proper in the adjacent regions, and vice versa. The highest current density is observed near the active spot of the monolithic electrode arc, resulting in a high temperature in this zone and its increased tip burnout. Specific resistive electrical losses in the cored electrode are smaller than those in the monolithic electrode by approximately 63 %. As the electrical losses are proportional to the square of current, it can be predicted that the current load in the cored electrodes can be raised by approximately 7–8 % during melting until the electrical losses in the cored and monolithic electrodes are equalized. This will improve the efficiency of steel melting and power saving.

Figure 5 shows the curves of the change of current density along the electrode height (coordinate *z*) on the electrode axis of symmetry (curve *1*), on the interface of the core and the electrode body (curve *2*), and on the electrode surface (curve *3*): in Figure 5, *a* for the cored electrode, and in Figure 5, *b* for the monolithic electrode. The humps on the curves coincide with the regions of the nipple location.

Figure 6 presents the curves of the change in the current density in the radial direction (coordinate *r*) at different height (sections 1–5, see Figure 4): in Figure 6, *a* in the cored electrode, in Figure 6, *b* in the monolith-

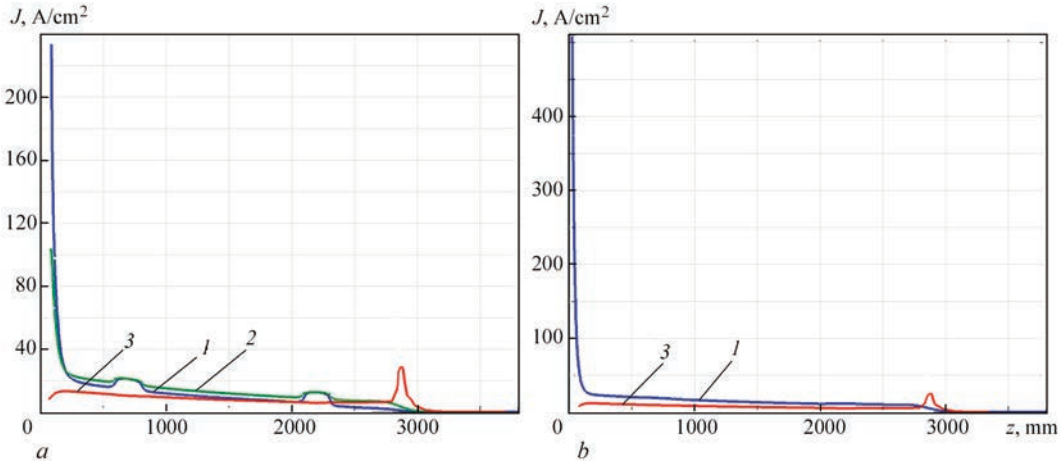

Figure 5. Curves of current density along the electrode height (coordinate *z*) on the electrode axis of symmetry (curve *1*), at the core and electrode body interface (curve *2*), on the electrode surface (curve *3*) in the cored electrode (*a*); in the monolithic electrode (*b*)

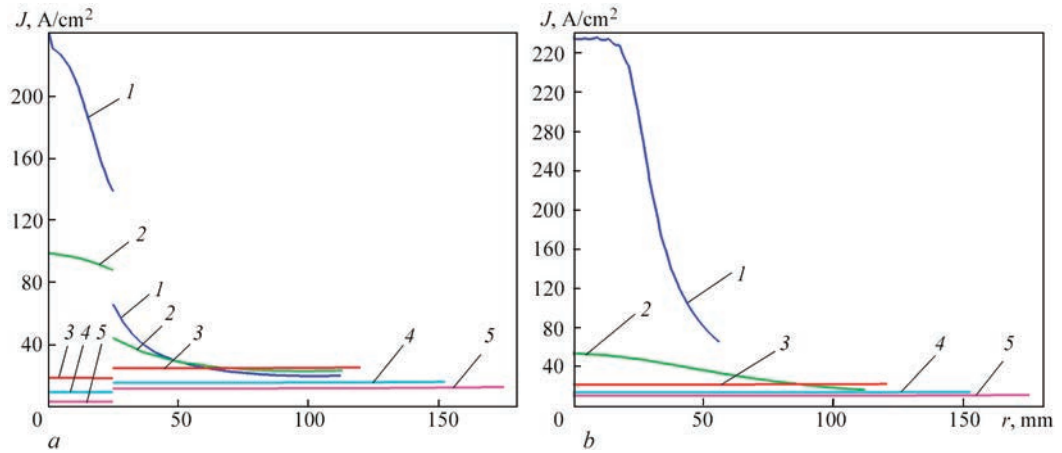

Figure 6. Curves of current density in the radial direction (coordinate *r*) at different height (sections 1–5, see Figure 4) in the cored electrode (*a*), in the monolithic electrode (*b*)

ic electrode. Breaks on the curves in Figure 6, *a* in the cored electrode coincide with the interfaces of the core and body of the electrode, which have different values of the specific electrical resistances.

Distribution of the current density in the electrodes in Figure 5 and 6 also correlates with the values of their specific electrical resistances at different temperatures (Figure 1). It is clearly visible that significant values of the current density are observed closer to the lower electrode tips, which are by an order of magnitude higher than over the greater length of the electrodes.

Figure 7 gives the temperature curves in the radial sections (coordinate *r*) at different heights (sections

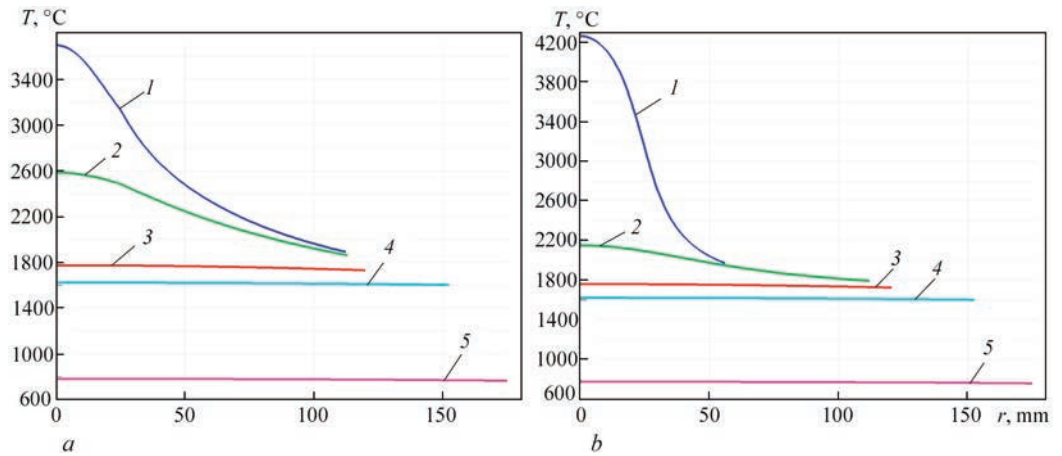

Figure 7. Curves of temperature in the radial direction (coordinate *r*) at different height (sections 1–5, see Figure 4) in the cored electrode (*a*), in the monolithic electrode (*b*)

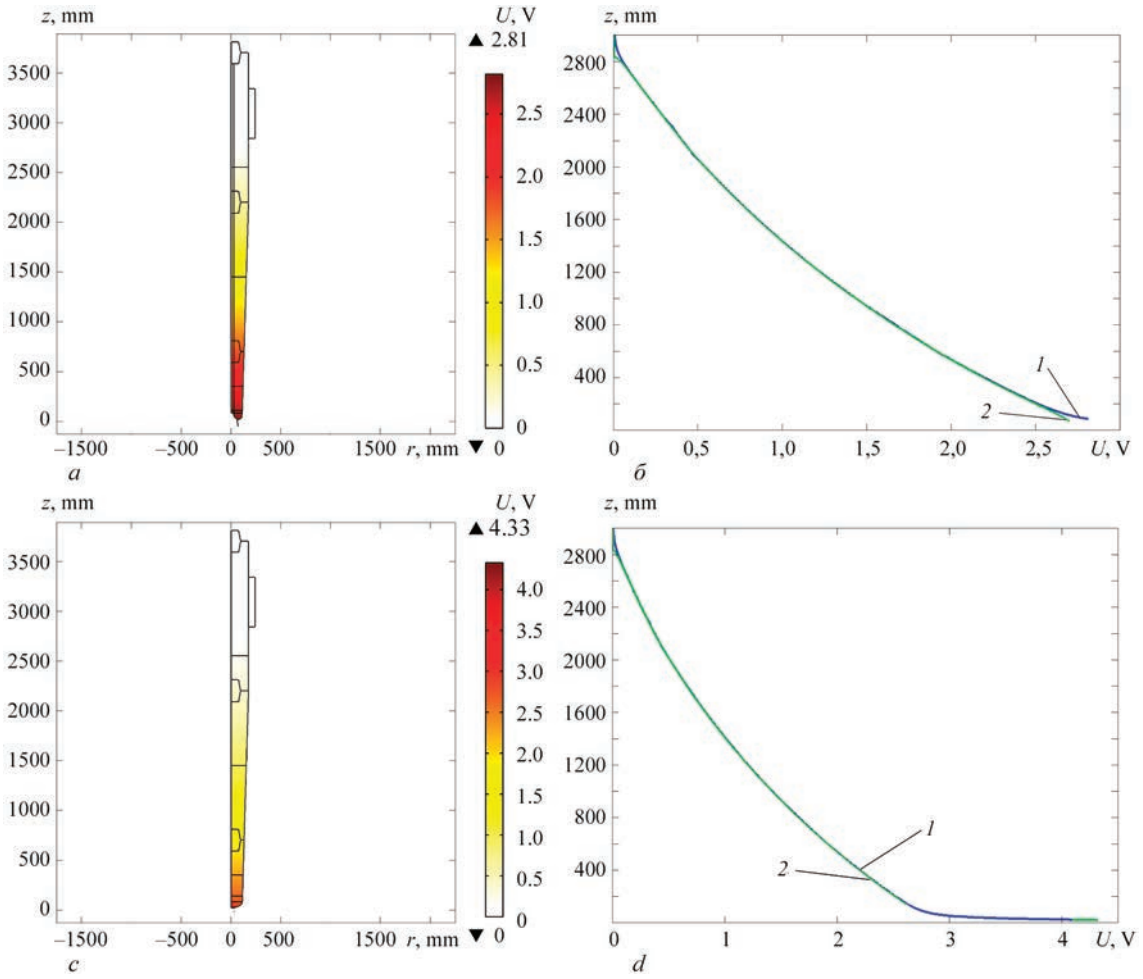

Figure 8. Electric potential distribution in the cored electrode body (*a*) and curves of electric potential along the electrode height (coordinate *z*) on the electrode axis of symmetry (curve *1*) and on the rectilinear side surface (curve *2*) (*b*); similar data for the monolithic electrode (*c*) and (*d*)

1–5, see Figure 4): in Figure 7, *a* in the cored electrode, in Figure 7, *b* in the monolithic one.

Figure 8, *a* presents the calculated distribution of the electrical potential (effective values) in the cored electrode body, and Figure 3, *b* shows the curves of electrical potential along the electrode height (coordinate *z*) on the electrode axis of symmetry (curve *1*) and on the rectilinear side surface (curve *2*). Figure 8, *c* and *d* are the same in the monolithic electrode. The electrical potential over the greater length of the cored electrode is higher than in the monolithic one, in connection with the fact that the electrical resistance of the considered core composition at temperatures close to 1900 °C, is greater than that of the monolithic electrode.

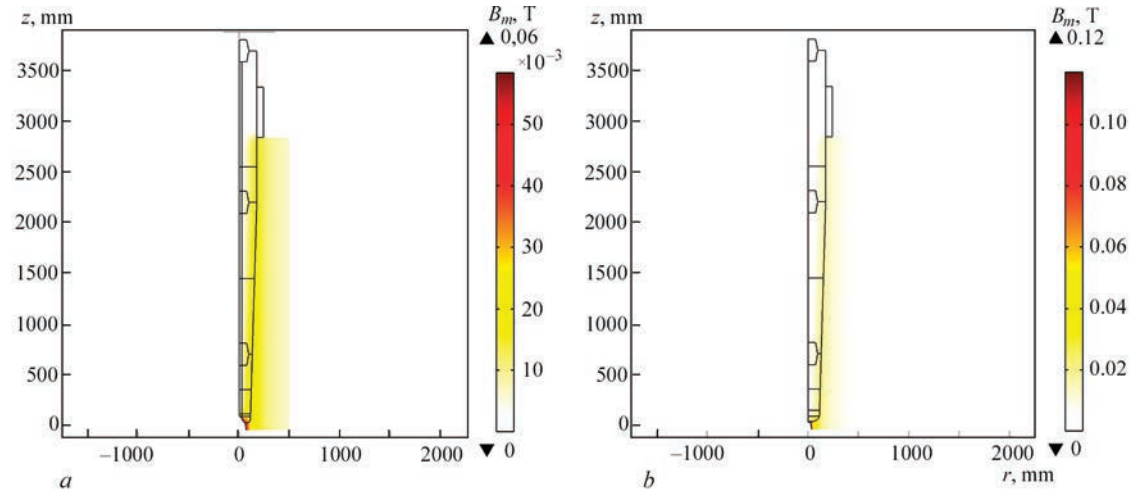

Figure 9. Distribution of magnetic induction for the cored electrode (*a*); for the monolithic electrode (*b*)

Figure 9, *a* shows the distribution of magnetic induction (amplitude values) for the cored electrode, and Figure 9, *b* is the same for the monolithic electrode. Greater values of magnetic induction are observed near the lower electrode tips.

Conducted calculations show the significant advantages of cored electrodes over the monolithic ones in terms of resource and energy saving during AC operation of the furnace. This is confirmed by multiple melts of the structural and corrosion-resistant steels in industrial steelmaking AC arc furnaces of 50–60 t capacity under the conditions of A.M. Kuzmin Electrometallurgical plant "Dniprospetzstal" (PJSC "Dniprosptezstal"), Ukraine.

Further studies should be devoted to more profound investigation of electromagnetic, thermal and thermochemical processes in the cored electrodes and improvement of the mathematical model, in particular allowing for simultaneous operation of the three electrodes of three-phase AC furnace.

CONCLUSIONS

1. A mathematical model was developed for numerical modeling of the electromagnetic and thermal processes in the graphitized cored (composite) and monolithic electrodes of the steelmaking AC arc furnaces, which are separated from the three-electrode system of the three-phase furnace.

2. The model allows determination of the distribution of the electromagnetic and temperature fields, electrical potential and current density in the electrodes, plotting the dependencies of the mentioned characteristics on a number of parameters taking into account the temperature dependencies of the specific electrical resistances of the core and electrode body.

3. For the cored electrode the value of the core electrical resistance at temperatures approximately up to 1900 °C is greater than the resistance of the graphitized electrode body. Accordingly, the resistance of a cored electrode region at these temperatures is higher than that of a similar region for the monolithic electrode. With temperature rising above the specified level, the core electrical resistance becomes smaller than the resistance of the graphitized electrode body, and the cored electrode resistance in such a region becomes smaller than that of a similar region of the monolithic electrode.

4. In the performed analysis it is taken into account that the AC arc on the cored electrode is defocused (its diameter is approximately equal to 1/2–3/4 of the electrode tip diameter), spatially stable, elastic, highly stable in a wide range of lengths and electrical modes, it has high thermal inertia and lower temperature. Now, in the monolithic electrode, the arc is concentrated, the arc active spot is small, and it constantly migrates over the electrode tip surface, burning it out and overheating the surface of the melt, leading to intensification of evaporation of the main and alloying elements from it.

5. It is shown that the current in the area of the arc active spot in the cored electrode (spot diameter based on experimental data is taken equal to 115 mm) flows relatively uniformly through its enlarged area, has lower density, compared to the monolithic electrode, and heating of the electrode lower part by currents is not as significant, as that in the monolithic electrode, where the current is concentrated in the arc active spot of a small area (with 50 mm diameter taken from the experiments).

6. In the case of the variable electric current flowing through an electrode separated from the furnace and the arc, which is located in open air at the temperature of 20 °C, the electrical losses and the temperatures in the cored electrode are lower than those in the monolithic one, allowing prediction of a higher energy efficiency of the cored electrodes, compared to the monolithic ones, as well as smaller burnout losses of the core material, and their higher resource effectiveness, accordingly. The temperature of the cored electrode lower part was equal to 544 °C, and that of monolithic electrode was 1387 °C. The total specific resistive electrical losses in the entire electrode volume under the same conditions (outside of the furnace) and with effective current value of 11 kA are equal to 0.1094 W/cm^3 for the cored electrode, and 0.2113 W/cm^3 for the monolithic one. Two times higher losses in the monolithic electrode are due to current concentration near the contact simulating the arc active spot.

7. Under the condition of thermal impacts on the electrode of the active arc spot (4440 °C for the monolithic electrode, T_0 = 4000 °C for the cored electrode), melt, furnace gases and furnace walls the calculated total specific resistive electrical losses in the entire volume of the studied cored electrode were equal to 0.1417 W/cm^3, and they are smaller than those in the monolithic electrode (0.3804 W/cm^3) approximately by 63 %. It can be predicted that the current load in the cored electrodes during melting can be increased by approximately 7–8 % up to equalizing of electric losses in the cored and monolithic electrodes, which will increase the steel making productivity and will ensure energy saving.

8. Based on the results of the conducted calculation with the simplifications and assumptions accepted in the mathematical model, it can be stated, that the cored electrodes have smaller electrical losses, lower temperature of the electrode working tip, compared

to monolithic electrodes, making the first more energy- and resource-efficient. This is also confirmed in practice during application of this type of electrodes in industrial steelmaking AC arc furnaces under the conditions of A.M. Kuzmin Electrometallurgical Plant "Dniprospetzstal".

REFERENCES

1. Rymar, S.V., Bogachenko, O.G., Honcharov, I.O. et al. (2023) Mathematical modeling of electric and thermal processes in graphitized wick electrodes for dc arc steelmaking furnaces. *Suchasna Elektrometalurhiya*, **3**, 28–39 [in Ukrainian]. DOI: https://doi.org/10.37434/sem2023.03.05
2. Paton, B.E., Bogachenko, O.G., Kiyko, S.G. et al. (2021) Experience of application of graphitized wick electrodes in industrial steel-making AC furnace. *Suchasna Elektrometalurhiya*, **1**, 48–53 [in Ukrainian]. DOI: https://doi.org/10.37434/sem2021.01.06
3. Paton, B.E., Lakomsky, V.I. Galinich, V.I., Mishchenko, D.D. (2011) Cored electrodes of electric arc furnaces. *Chyorn. Metally*, **5**, 13–15 [in Russian].
4. Bogachenko, A.G., Mishchenko, D.D., Braginets, V.I. et al. (2016) Saving of electric power at the arc steel melting furnaces of direct current with graphitized cored electrodes. *Sovremennaya Elektrometallurgiya*, **1**, 58–64 [in Russian]. DOI: https://doi.org/10.15407/sem2016.01.09
5. Bogachenko, O.G., Mishchenko, D.D., Goncharov, I.O. (2023) Application of graphitized wick electrodes in DC arc steel furnaces. *Suchasna Elektrometalurhiya*, **1**, 53–61 [in Ukrainian]. DOI: https://doi.org/10.37434/sem2023.01.07
6. Bogachenko, O.G., Chernyakov, A.V., Goncharov, I.O. et al. (2024) Application of graphitized cored electrodes in 50 ton steel melting AC arc furnace of DSV-50 type. *Suchasna Elektrometalurhiya*, **1**, 32–39 [in Ukrainian]. DOI: https://doi.org/10.37434/sem2024.01.04
7. Pashatsky, N.V., Molchanov, E.A. (1998) Thermal state of electrodes of arc furnaces. *Izv. Vuzov. Chyorn. Metallurgiya*, **5**, 24–26 [in Russian].
8. Kozhukhov, A.A., Mereker, E.E., Sazonov, A.V. (2008) To problem of temperature distribution in electrodes of arc steel-making furnace. *Izv. Vuzov. Chyorn. Metallurgiya*, **9**, 7–10 [in Russian].
9. Mokhov, V.A., Yachikov, V.M. (2012) Modeling of thermal state of arc furnace graphitized electrode taking into account evaporation cooling. *Elekrometallurgiya*, **11**, 35–41 [in Russian].
10. Gasik, M.M. (2024) Simulation of electric arc mode of electric furnace and analysis of its operation in real time. *Suchasna Elektrometalurhiya*, **2**, 20–24 [in Ukrainian]. DOI: https://doi.org/10.37434/sem2024.02.03
11. Krikent, I.V., Krivtsun I.V., Demchenko, V.F., Pyptyuk V.P. (2013) Numerical modeling of high-current arc discharge in DC ladle-furnace unit. *Sovremennaya Elektrometallurgiya*, **3**, 45–50.
12. Lakomsky, V.I. (1997) Oxide cathodes of electric arc. Zaporozhie, Izd-vo Internal, 192 [in Russian].

ORCID

I.V. Krivtsun: 0000-0001-9818-3383,
S.V. Rymar: 0000-0003-0490-4608,
O.G. Bogachenko: 0000-0002-3306-6626,
I.O. Honcharov: 0000-0003-2915-0435,
I.O. Neilo: 0009-0003-4771-3630,
R.S. Hubatyuk: 0000-0002-0851-743X.
O.T. Zelnichenko: 0009-0006-4604-4561

CONFLICT OF INTEREST

The Authors declare no conflict of interest

CORRESPONDING AUTHOR

S.V. Rymar
E.O. Paton Electric Welding Institute of the NASU
11 Kazymyr Malevych Str., 03150, Kyiv, Ukraine.
E-mail: elmag@paton.kiev.ua

SUGGESTED CITATION

I.V. Krivtsun, S.V. Rymar, O.G. Bogachenko, I.O. Honcharov, I.O. Neilo, R.S. Hubatyuk, O.T. Zelnichenko (2026) Mathematical modeling of electrical and thermal processes in a graphitized cored electrode for alternating current arc steelmaking furnaces. *The Paton Welding J.*, **02**, 3–13. DOI: https://doi.org/10.37434/tpwj2026.02.01

JOURNAL HOME PAGE

https://patonpublishinghouse.com/eng/journals/tpwj

Received: 05.12.2025
Received in revised form: 14.01.2026
Accepted: 25.02.2026